Original Article

Design and Development of Dual Functional Colon Targeted Eudragit/Chitosan Nanoparticles: A QbD Approach

Priyadarshini Patel[1,*], Tejas Patel[2]

[1]Department of Pharmaceutics, ROFEL Shri G. M. Bilakhia College of Pharmacy, Vapi, Gujarat, INDIA.
[2]Department of Pharmaceutics, Dharamsinh Desai University, Nadiad, Gujarat, INDIA.

ABSTRACT

Aim: The goal of this study was to develop colon-targeted nanoparticulate systems of the anti-inflammatory agent Quercetin (QU) and evaluate the formulation for various parameters that would allow the active ingredient to be released at a predetermined time and location with better pharmaceutical and therapeutic properties. **Materials and Methods:** Quercetin-loaded chitosan nanoparticles were formulated for this purpose using the ionic gelation method by employing Central Composite Design. To coat Eudragit S 100 (ES 100) on an optimised formulation of quercetin loaded chitosan nanoparticles (QLCN), the oil in oil solvent evaporation process was used. Particle size (PS), polydispersity index (PDI), scanning electron microscopy (SEM), and drug release (% DR) were evaluated to characterize the nanoparticles. **Results:** Quercetin loaded chitosan nanoparticles has an average PS 114.2 ± 1.42 nm and polydispersity index 0.396 ± 0.02, whereas Eudragit coated nanoparticles shows PS 330.2 ± 0.40 nm and polydispersity index 0.412 ± 0.02. Surface morphology of prepared nanoparticles were confirmed using SEM. According to an *in vitro* drug release analysis of nanostructured formulations, the ES 100 coating on QLCN inhibits the release of quercetin in the upper gastrointestinal system, demonstrating good colon drug targeting. **Conclusion:** According to an *in vitro* release study of nanoparticle formulations, the ES 100 coating on QLCN limits the release of quercetin in the upper gastrointestinal system, demonstrating effective colon drug targeting.

Keywords: Anti-inflammatory agent, Ionic gelation method, Central composite design, Quercetin loaded chitosan nanoparticles, Eudragit S 100, Colon targeting.

INTRODUCTION

For thousands of years, plants have formed the foundation of many traditional medicine systems around the world, and they stand to be the only new source of structurally significant chemical compounds that lead to revolutionary drug discovery. The discovery of new anti-inflammatory and anti-allergic agents from the vast medicinal plant capital is becoming more intense these days.[1] A myriad of bioactive components have also been shown to have anti-inflammatory characteristics.[2]

Quercetin is a flavonoid found copiously in basically all edible fruits and vegetables. The average Western diet contains approximately 15 milligrams of quercetin. For example, Figures, blueberries, cranberries, and red onions are predicted to contain 5, 8, 15, and 39 mg of quercetin aglycone per 100 g of fresh weight of eatable part, respectively.[3,4]

There is rising evidence showing that quercetin encompasses a great therapeutic potential to forestall and treat various chronic diseases, including cardiovascular and neurodegenerative diseases, still as cancer.[5-9] Quercetin has been shown to own beneficial health effects in an exceedingly sort of cellular and animal models, similarly as in humans, by modulating the signalling pathways and gene expression involved

Submission Date: 21-03-2022;
Revision Date: 09-06-2022;
Accepted Date: 08-08-2022.

DOI: 10.5530/ijper.56.4.187

Correspondence:
Mrs. Priyadarshini Patel
Department of Pharmaceutics, ROFEL Shri G. M. Bilakhia College of Pharmacy, Vapi-396191, Gujarat, INDIA.
E-mail: patelpriyadarshi-ni1990@gmail.com

www.ijper.org

in these processes.[10] Quercetin, with daily suggested doses of 200-1200 mg, may also be taken as a dietary supplement and even as a nutraceutical via functional foods with levels ranging from 10-125 mg per serving. Evidence on the safety of using quercetin as a dietary supplement and adding it to diet is substantial.[11-12] There has been much attention given to the potential for health promotion overall flavonoid properties and of particularly quercetin. Various epidemiological research reports an inverse correlation between the consumption of flavonoids and cardiovascular disease threats and incidence of colorectal and lung cancers. Such advantageous effects were due to antioxidant Flavonoid Capacities.[13]

Colon targeting refers to formulations that restrict the encapsulated compound's decomposition, elimination, and/or absorption in the stomach and small intestine until it enters the lower digestive tract, resulting in increased local delivery to the colonic region.[14] Nevertheless, because the colon is situated in the distal area of the digestive tract, it is difficult to design a delivery system that can survive the passage to this particular region. Factors such as the GI stability of certain polyphenols, the physiological barrier of the colon, and the features of the encapsulating material must all be carefully studied when designing colon delivery techniques for polyphenols.[15]

Polyphenols are well recognised for their low oral bioavailability, with just 5-10% of the pure form being absorbed in the upper GI tract; several promising nano/microencapsulation-based methods have been designed to improve polyphenols' absorption efficiency by enhancing their dissolution rates and solubility.[16] Conversely, formulations for colon-targeting should be able to avoid or minimize the release and depletion of polyphenols in the upper GI tract, and payload release should be triggered until the carrier reaches the colon.[17] In an effort to overcome constraints on traditional formulations, recent pharmaceutical advancements have employed nanotechnology to the design of oral dosage forms. Nano-delivery systems have been proven to have comparable or better therapeutic effectiveness at lower drug concentrations when compared to conventional formulations.[18-19] Improved oral drug delivery technology has substantially increased drug bioavailability in the colon, indicating that all these formulations are successful in precisely accessing and releasing drugs in the colon.[20] Nanoparticles are a form of colloidal drug delivery system which includes particles with a diameter range from 10 to 1000 nm. Because of their small size, nanoparticles may also penetrate profoundly into target tissue, which may be useful for the treatment of colonic disease.[21] NPs also have the potential for alteration of drug properties, including stability, solubility and immunogenicity. In addition, surface customization of NPs enables targeted and controlled release of drug to optimize drug concentration at the site of inflammation for a extended duration of time, limiting systemic adverse effects.[22-23]

Chitosan, a polycation with an apparent pKa 6.1-7.3 at acidic pH, is a plentiful natural polysaccharide found in Crustacean and obtained from N-deacetylation of chitin. Chitosan presents numerous benefits in terms of oral colon drug delivery, including being biodegradable, biocompatible, non-toxic, non-immunogenic, and colonically digested. In gentle situation chitosan can also form nanoparticles with polyphosphate through ionotropic gelation for protein and peptide drug loading.[24-26]

Eudragit is a pH-dependent, soluble polymer composed of methacrylic acid and methyl methacrylate (1:2) that is utilised for colon-specific drug administration.[27] In this study, ES 100 was employed as an enteric coating to shield chitosan nanoparticles from degradation in the gastric medium of the stomach and upper intestine, which can aid in drug release and absorption in the colon.[26-28]

The ES 100 coated chitosan nanoparticles co-loaded with quercetin were developed in this work to protect quercetin against degradation in upper gastrointestinal tract, which may then pave the way for the release and absorption of drugs in the colon.

MATERIALS AND METHODS

Materials

Chitosan (low molecular weight, viscosity 20–300 cP, deacetylation ≥ 95% and sodium tripolyphosphate (STPP) were procured from Sigma-Aldrich. Quercetin was purchased from Sisco Research Laboratories, Maharashtra, India. Syringe filter, dialysis bag (cut-off molecular weight 12000 Da were procured from Himedia, Mumbai, India. Glacial Acetic acid, Sodium hydroxide pellets, HCl, Methanol, Potassium dihydrogen phosphate and Disodium hydrogen phosphate were obtained from Thomas baker, Mumbai, India. Eudragit S 100 was a munificent gift of Evonik India Pvt. Ltd, Mumbai. All materials used were of analytical grade.

Methods

Formulation and Optimization of Eudragit Coated Chitosan Nanoparticles

Drug Excipient Compatibility Study

Here, the excipients were chosen on the basis of preformulation study of drugs. All excipients selected

here are listed in GRAS and IIG. The shimadzu FTIR spectrophotometer was used to examine the compatibility of the drugs and excipients in a physical mixture (1:1). Before testing, the sample chamber was filled with nitrogen gas and dry desiccant to eliminate any moisture content presence. The sample pellets were made by using a dry KBr (IR grade) system of approximately 10-15 percent. Powders were ground in a small-sized mortar and pestle until the powder blend was fine and even. For the background and correction of the baseline, pure KBr powder was used. Samples were inserted into the sample holder. Then the specimen was transferred to the sample compartment. A shimadzu spectrophotometer was used to scan samples in the 4000-400 cm-1 region.[29]

Formulation and optimization of QU loaded nanoparticles of Chitosan

The CS-STPP nanoparticles were fabricated using the previously described method.[30-31] The CS was dissolved in acetic acid solution with continuous stirring until the solution was clear. STPP aqueous solution had been prepared. The synthesis of CS-STPP nanoparticles commenced spontaneously following the addition of STPP solution to a CS solution with stirring at room temperature through the ionic gelation mechanism instigated by STPP. For the fabrication of QU loaded CS-STPP nanoparticles, an ethanolic solution of QU (1 mg/ml) was added to STPP solution, which was then syringe dropped into CS solution and stirred at room temperature for 1 hr. Nanoparticles were collected by centrifugation at 5000 rpm for 20 min at 20°C, with the supernatants collected for drug content analysis and the remains were dialyzed with distilled water to eliminate unbound drug; the dialyzed formulation was then lyophilized and utilised for additional assessment.

Screening of Preliminary Factors

All of the samples were prepared at room temperature (28 ± 2°C). All these experiments were conducted at the same CS: STPP mass ratio of 4:1, 4.5 chitosan solution pH based on earlier research findings. 10 mg of drug was taken to prepare the nanoparticles. At room temperature (28 ± 2°C), all samples were prepared.

Stirring rate

A 0.1 percent w/v chitosan solution was formed in 1 percent v/v glacial acetic acid. The resultant solution was stirred for 30 min under continuous magnetic stirring at 600 RPM. The solution was then vacuum filtered using a 0.45 m filter. Using 4 N NaOH, the pH of the solution was attuned to 4.5. A 0.0625% w/v STPP solution was made and filtered using a 0.45 m filter. Following that, 6 mL of STPP solution was syringe dropped on 15 mL of chitosan solution under magnetic stirring for 60 min. Four samples were prepared, each with a different stirring rate (200rpm, 400rpm, 600rpm, and 800rpm). Particle size (PS), polydispersity index (PDI), and percent entrapment efficiency (% EE) were determined for prepared samples.

Acetic Acid Concentration

Chitosan solutions of 0.10 percent w/v in 1%, 1.5 percent, and 2 percent w/v glacial acetic acid were prepared. A 0.0625% w/v STPP solution was prepared and filtered. Three samples were prepared by varying acetic acid concentrations with magnetic stirring at 600 rpm for 60 min by syringe dropping of 6 ml STPP solution on 15 ml chitosan. PS, PDI, and % EE were determined for prepared samples.

STPP pH Adjustment

Two samples were produced by syringe dropping 6 ml 0.0625% w/v STPP solution on 15 ml 0.1% w/v chitosan solution in 1.5% v/v acetic acid for 60 min with magnetic stirring at 600 rpm. The pH of STPP was left unadjusted in one sample and modified to 4.5 (the same pH as chitosan solution) in the other using 0.1 N HCl. PS, PDI, and % EE were determined for prepared samples.

Screening of Crucial Factors

Based on the findings of the preliminary factors investigations, a stirring rate of 600 rpm and a concentration of 1.5% v/v acetic acid (6 ml STPP solution without pH modification on 15 ml chitosan solution) were adopted to conduct subsequent experiments.

CS: STPP Mass Ratio

By fluctuating the concentration of the STPP solution (0.1250%, 0.0830%, 0.0625%, 0.0500%, 0.0420%, and 0.0355% w/v), the CS: STPP mass ratio varied by 2:1, 3:1, 4:1, 5:1, 6:1, and 7:1. The pH of the chitosan solution was kept consistent at 4.5, and studies were conducted at room temperature. PS, PDI, and % EE were assessed for prepared samples.

Chitosan Solution pH

The pH of the chitosan solution was modified to 3.5, 4.0, 4.5, 5.0, and 5.5, using 4 N NaOH. The CS: STPP mass ratio was maintained constant at 4:1 throughout the experiments, which were conducted at room temperature. PS, PDI, and % EE were evaluated for synthesized nanoparticles

Amount of Drug

By introducing five separate amounts of QU (5, 7.5, 10, 12.5, 15 mg) into 0.0625% w/v 6 ml STPP solution, the drug concentration was changed. The chitosan solution pH was kept constant at 4.5, Chitosan: STPP ratio 4:1 was kept constant, and the experiments at room temperature were carried out. Prepared samples were evaluated for PS, PDI and % EE.

Design of Experiments for Studying Critical Factors

Quercetin-loaded chitosan nanoparticles were fabricated using the central composite design. The Chitosan: STPP mass ratio and the pH of the chitosan solution were chosen as independent variables. The response variables chosen were PS (Y1), PDI (Y2), and % EE (Y3). Based on the pre-optimization study that was carried out before the experimental design was applied, the levels were selected. All other variable for formulation and processing was kept equable during the experiments. Table 1 shows the translation of coded values of independent variables and the experimental design.

Enteric coating of nanoparticles

The above-prepared Quercetin-loaded chitosan nanoparticles (QLCN) were then coated with ES 100 through an oil-in-oil solvent evaporation technique. In 10 ml of coating solution, QLCN were dispersed, made by dissolving ES 100 in an acetone: ethanol mixture (1:2). The aforementioned dispersion was then dropped into light liquid paraffin (50 ml) comprising 1.5% w/v Span 80. The dispersion was held at room temperature for 180 min with agitation at 600 rpm before the organic phase was withdrawn under vacuum. To obtain ES 100 coated quercetin nanoparticles, the solution was rinsed with n-hexane (3 * 50 ml) to eliminate liquid paraffin and dried.[32-33] The core/coat ratios have been optimised to achieve spherical nanoparticles with smooth surface coating, as shown in Table 2.

Table 1: Dependant and independent variables used in factorial design.

Independent Variables	Variable level	
	Low (-1)	High (+1)
Chitosan: STPP mass ratio (X1)	3:1	6:1
pH of chitosan solution (X2)	4	5
DEPENDANT VARIABLES	**CONSTRAINS**	
Y1 = Particle size (nm)	Minimize	
Y2 = Polydispersity index	Minimize	
Y3 = % EE (Entrapment Efficiency)	Maximize	

Table 2: Core: coat ratios used to coat quercetin loaded chitosan nanoparticles.

Batch	Core: Coat ratio
F1	1:2
F2	1:3
F3	1:4
F4	1:5

Nanoparticles Characterization

% Loading capacity (%LC) and % Entrapment efficiency (%EE)[34-35]

The percentage of QU loaded in nanoparticles was measured after centrifuging the obtained nanoparticles for 1 hr at 10,000 rpm and quantifying the free drug content in the supernatant using an effective UV spectrophotometric method at a wavelength of 256.5 nm. Loading capacity in nanoparticles were determined by following equation:

$$\%LC = [\text{Weight of QU in NPs} / \text{Weight of NPs}] * 100$$

$$\%\ EE = [(\text{Weight of QU used} - \text{Weight of un-entrapped QU}) / \text{Weight of QU used}] * 100$$

Particle size (PS) and polydispersity index (PDI)

After being adequately diluted with distilled water, the average particle size and PDI were assessed using a Zetasizer at 25°C (Malvern Instrument Ltd., Worcestershire, UK).[36-37]

Surface Morphology Study

Scanning electron microscopy was used to inspect the particle morphology before and after the Eudragit S100 coating (SEM). The nanoparticles were deposited on aluminium stubs, sputtered with a thin Au/Pd layer, and studied using a scanning electron microscope.[38]

In vitro Drug Release

An *in vitro* drug release study of QU loaded chitosan nanoparticles and ES 100 coated chitosan nanoparticles was conducted in simulated gastrointestinal fluids, namely (a) in simulated gastric fluid (SGF) at pH 1.2 (0–2 h), (b) in simulated intestinal fluid (SIF) at pH 6.8 (2–5 hr), and (c) in simulated colonic fluid (SCF) at pH 7.4 (5–24 hr).

Pre-treated dialysis bags containing quercetin loaded chitosan nanoparticles and ES 100 coated chitosan nanoparticles were sequentially immersed in the

aforementioned dissolution media (100 ml) at 100 rpm with magnetic stirring at 37 ± 0.5°C for 24 hr. 1% v/v Tween 80 was added in dissolution media to aid in the solubilization of QU released from nanoparticles. Samples (2 ml) were collected at set intervals (0.5, 1, 2, 3, 4, 5, 6, 8, 12, and 24 hr) and replenished with the identical volume of the corresponding dissolution media after apiece sample to preserve the sink condition. Following proper dilution, the samples were centrifuged at 5000 rpm for 20 min, the supernatant was filtered via 0.22 membrane filter, and the filtrate was submitted for spectrophotometry.[39]

Determination of Release Kinetics

In vitro drug dissolution to envisage *in vivo* bio performance may be contemplated pragmatic design of controlled release formulations as qualitative and quantitative alterations in a formulation can impact drug release and *in vivo* performance. As a result, release kinetic models should be determined that reflect the entire drug release through the formulations. To forecast the mechanism of release of drug from QU charged chitosan nanoparticles and ES 100 coated chitosan nanoparticles, model-dependent techniques were utilised (zero order, first order, Higuchi, Korsmeyer – Peppas models), and the best model was picked utilizing correlation coefficient.[40-41]

RESULTS AND DISCUSSION

Drug excipient compatibility study in physical mixture of drug with excipients (1:1 ratio)

Drug excipient compatibility study of QU with selected excipients was performed by FTIR spectroscopy. Results are shown in Figure 1.

1. QU
2. QU + Chitosan
3. QU + Sodium tripolyphosphate
4. QU + Eudragit S 100

Quercetin showed distinctive peaks at 3320 cm^{-1} (-OH stretching), 1664 cm^{-1} (C=O stretching), and 1522 cm^{-1} (C=C stretching) according to FTIR spectroscopy. Furthermore, absorption bands associated to the angular deformation of C=CH of aromatic compounds were observed in the range of 650 to 1000 cm^{-1}[29].[42]

In FTIR spectra of physical mixtures (PM) of QU with chitosan, STPP, and ES 100 individually, all of the drug's distinctive peaks were found, as shown in Figure 1. FTIR study showed that the excipients and drug were not interacting with each other.

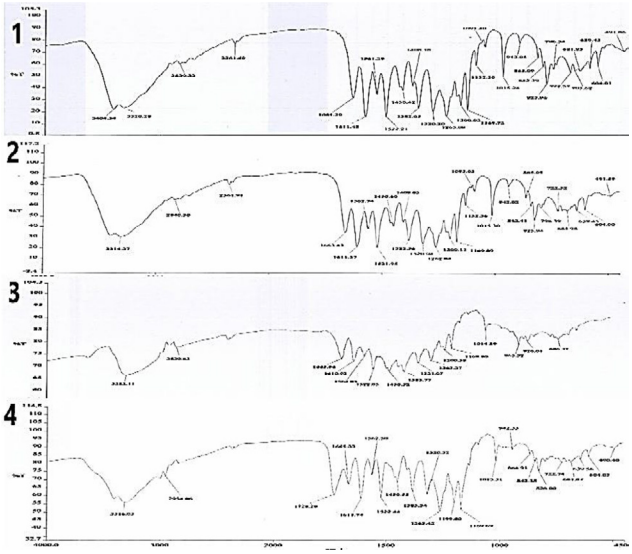

Figure 1: FTIR spectra of 1) QU, 2) QU + Chitosan, 3) QU + STPP, 4) QU + ES 100.

Investigation of Preliminary Factors

Selection of Stirring rate

The stirring rate of 600 rpm generated the smallest particle size and the least polydispersity index, as seen in Table 3.

This slow rate provides for the best possible contact between the chitosan solution and the STPP, which can aid in the formation of nanoparticles. Subsequent experiments therefore conducted at 600 rpm.

Selection of Stirring time

Four samples of nanoparticles were prepared as described in the Table 3, at different stirring time. All the other parameters kept unchanged. The prepared batches were then tested for PS, PDI, % EE and LC. The B6 and B7 lots showed minimal PS, PDI and % LC while the B7 and B8 showed maximum % EE. Hence, the encapsulation efficiency of quercetin can be assumed to be time-dependent for the complete interaction between quercetin and CS. As a result, all of the subsequent batches of nanoparticles were prepared using a stirring time of 60 min.

Selection of Acetic Acid Concentration

The batches B9, B10 and B11 had been prepared by altering the concentrations of acetic acid used for chitosan dissolution. By increasing the concentration from 1 to 1.5% the PS and PDI decreases. Higher acetic acid concentration, however, led to larger and more polydispersed particles. This could be due to better chitosan dissolution and more effective breakage of chitosan aggregates. Consequently, 1.5% of acetic acid was used for further studies.

Table 3: Evaluation parameters for nanoparticles of preliminary batches (*n*=3, mean ± SD).

Runs	Batch	Factor PS		Evaluation parameters			
				PDI	%EE	%LC	
1	B1	Stirring Rate (RPM)	200	249.6 ± 2.43	0.643 ± 0.01	25.2 ± 1.25	9.10 ± 0.62
2	B2		400	189.3 ± 1.39	0.542 ± 0.03	78.9 ± 1.83	11.93 ± 0.35
3	B3		600	125.9 ± 1.42	0.388 ± 0.03	81 ± 1.80	18.47 ± 0.15
4	B4		800	181.6 ± 1.31	0.706 ± 0.04	52.6 ± 1.91	14.93 ± 0.65
5	B5	Stirring Time (min)	30	136.3 ± 1.05	0.589 ± 0.02	69.4 ± 1.10	16.73 ± 0.40
6	B6		45	123.7 ± 2.09	0.403 ± 0.01	75.4 ± 1.30	17.20 ± 0.36
7	B7		60	125.3 ± 0.95	0.324 ± 0.01	82.2 ± 1.15	19.23 ± 0.55
8	B8		90	131.2 ± 1.59	0.643 ± 0.02	81.1 ± 1.70	15.80 ± 0.78
9	B9	Acetic Acid Concentration (%V/V)	1	126.3 ± 1.95	0.423 ± 0.02	78.6 ± 1.01	17.60 ± 0.30
10	B10		1.5	122.4 ± 1.18	0.389 ± 0.02	81.1 ± 1.75	18.63 ± 0.64
11	B11		2	304.2 ± 0.85	0.633 ± 0.01	79.3 ± 1.05	12.10 ± 0.20
12	B12	STPP pH Adjustment	4.5	125.6 ± 1.78	0.356 ± 0.01	83.2 ± 1.44	18.50 ± 0.36
13	B13		Unadjusted	123.8 ± 1.06	0.349 ± 0.03	81.6 ± 1.41	18.60 ± 0.50
14	B14	CS: TPP Mass Ratio	2: 1	348.3 ± 0.85	0.618 ± 0.02	65.2 ± 1.01	8.20 ± 0.26
15	B15		3: 1	135.1 ± 0.44	0.425 ± 0.01	75.3 ± 1.21	13.40 ± 0.53
16	B16		4: 1	123.7 ± 0.80	0.381 ± 0.01	77.5 ± 0.95	17.37 ± 0.61
17	B17		5: 1	118.9 ± 1.70	0.419 ± 0.02	83.2 ± 1.27	19.47 ± 0.21
18	B18		6: 1	128.3 ± 0.90	0.346 ± 0.02	81.4 ± 1.65	15.10 ± 0.70
19	B19		7:1	289.7 ± 0.75	0.516 ± 0.01	59.2 ± 1.25	10.77 ± 0.61
20	B20	Chitosan Solution pH	3.5	202.3 ± 0.65	0.567 ± 0.02	70.8 ± 1.50	10.53 ± 0.32
21	B21		4	136.7 ± 0.76	0.306 ± 0.02	76.1 ± 1.55	13.53 ± 0.35
22	B22		4.5	121.6 ± 1.85	0.427 ± 0.01	78.9 ± 1.76	18.57 ± 0.65
23	B23		5	141.2 ± 2.01	0.367 ± 0.02	83.2 ± 1.01	16.90 ± 0.87
24	B24		5.5	303.9 ± 0.98	0.613 ± 0.02	75.3 ± 1.35	11.47 ± 0.38
25	B25	Amount of Drug (mg)	5	119.8 ± 1.95	0.418 ± 0.01	69.2 ± 2.10	21.40 ± 0.26
26	B26		7.5	122.1 ± 0.90	0.345 ± 0.02	72.1 ± 0.90	20.17 ± 0.31
27	B27		10	128.2 ± 2.23	0.314 ± 0.01	80.2 ± 1.80	18.90 ± 0.36
28	B28		12.5	165.3 ± 1.40	0.328 ± 0.01	76.3 ± 1.07	16.13 ± 0.25
29	B29		15	256.4 ± 1.65	0.473 ± 0.01	63.2 ± 1.76	13.60 ± 0.46

Selection of STPP pH

Because no noteworthy differences were perceived between the PS, PDI, % EE, and % LC obtained for nanoparticles produced from adjusted and unadjusted STPP solutions, the unadjusted STPP solution was utilised in the subsequent studies.

Investigation of Crucial Factors

Selection of CS: STPP mass ratio

It is evident from Table 3 varying the CS: STPP mass ratio from 2:1 to 7:1 six different batches had been prepared. The effects on PS, PDI, % EE and % LC were found to fluctuate. These findings supported the use of statistical modelling to achieve the optimal particle size, PDI and % EE.

Selection of pH of Chitosan Solution

Batches B20 to B24 were prepared by altering the pH of chitosan solution. Fluctuating effects were observed on PS and PDI. Although % EE and % LC increased upon increasing the pH of chitosan solution. (Table 3)

Selection of Amount of drug

NPs is prepared by the addition of different concentration of quercetin. Table 3 shows the comparative impact of concentration of the drug on PS, PDI, % EE and % LC. According to the findings, the addition of Quercetin to chitosan has contributed to an increase in the size of nanoparticles. Nanoparticles did not grow considerably in size at concentrations up to 10 mg, but there was a transition in size occurred when the drug concentration was raised from 10 to 15 mg. The % EE and % LC

increased to 10 mg but then reduction was observed in both as the concentration increased.

From the results of preliminary batch evaluation parameters, it was noted that CS: STPP mass ratio and pH of chitosan solution, these two factors had fluctuating effects on PS, PDI and % EE.

These findings necessitated the application of statistical modelling to attain the required particle size, PDI, and % EE domains for both variables, in order to illustrate the relevance of each and examine their relationships.

Optimization of Nanoparticles using Central Composite Design

Model fitting and statistical analysis

The influence on dependent variables was investigated using a central composite experimental design with two independent variables at three levels. As outlined in Table 4, a total 9 formulations were developed conferring to the experimental design and evaluated further for responses such as PS, PDI, % EE, % LC, and Zeta potential.

One-way Analysis of variance (ANOVA) for dependant variables

For all the 9 batches response variables, PS (Y1) and PDI (Y2) and % EE (Y3) showed wide variations from 112.6 ± 1.15 to 210.3 ± 1.25 nm, 0.346 ± 0.02 to 0.513 ± 0.02 and 73.1 ± 1.10 to 82.6 ± 1.12 respectively as depicted in Table 4, displaying a strong impact of independent variables (X1 and X2) on the selected responses.

Multi linear regression analysis was used to construct mathematical models and establish coefficients of second order polynomial equations for PS (Y1), PDI (Y2), and % EE (Y3). The equations were discovered to be quadratic with interaction terms. The polynomial coefficients were well-fitting to the data, with R^2, 0.9941, 0.9836, and 0.9960 for Y1, Y2, and Y3 correspondingly.

$$Y1 = 112.60 - 7.32\,X1 + 11.22\,X2 + 5.37\,X1X2 + 43.13\,X1^2 + 11.35\,X2^2$$

$$Y2 = 0.4010 - 0.0295\,X1 + 0.0136\,X2 - 0.0002\,X1X2 + 0.0328\,X1^2 - 0.0212\,X2^2$$

$$Y3 = 81.20 + 1.09\,X1 + 0.9252\,X2 + 0.2750\,X1X2 - 3.33\,X1^2 + 0.0187\,X2^2$$

The one-way ANOVA test was utilised to authenticate the appropriateness of these models. Table 5 summarises the findings. Y1, Y2, and Y3 had P values of 0.0015, 0.0070, and 0.0009, correspondingly. It may be inferred that the Y1, Y2, and Y3 findings closely matched the model. In the context of the central composite design, the findings were quite substantial.

The correlation between the dependent and independent variables was elucidated further by means of response surface plot. For all noted dependent variables, contour plots (2-D) and surface plots (3-D) were used to optimise the formulation. The Design expert 12 software was used to construct contour plots and surface plots. These plots are useful for examining the impact of two variables on a response at the same time. The other variables in all of the graphs were kept at a constant level. Figure 2 shows several contour plots and response surface plots for Y1, Y2, and Y3, sequentially.

From Figure 2, it was observed that as the CS: STPP mass ratio increases particle size decreases to a certain point minimum than increases. It has been found that the particle size of the nanoparticles rises as the pH of the chitosan solution increases. So as the CS: STPP mass ratio increases PDI declines to a certain point minimum then increases. Similar effect was observed upon increasing the pH of the chitosan solution. As the CS: STPP mass ratio increases % EE rises to a certain point maximum than decreases. The % EE of the nanoparticles has been observed to increase when the pH of the chitosan solution rises.

Table 4: Evaluation parameter of QU loaded nanoparticles of CCD batches (n=3, mean ± SD).

Batches	CS: STPP mass ratio	pH of chitosan solution	PS (nm)	PDI	%EE Mean ± SD (n = 3)	%LC Mean ± SD (n = 3)	Zeta potential
C1	**3**	**4**	165.2 ± 1.65	0.423 ± 0.01	76.2 ± 1.76	15.73 ± 0.57	26.9 ± 1.54
C2	**6**	**4**	140.3 ± 0.90	0.362 ± 0.01	78.1 ± 1.36	16.33 ± 0.90	24.1 ± 1.07
C3	**3**	**5**	181.6 ± 0.75	0.451 ± 0.01	77.3 ± 1.14	16.57 ± 0.50	28.4 ± 1.12
C4	**6**	**5**	178.2 ± 0.40	0.389 ± 0.02	80.3 ± 1.62	17.10 ± 0.85	23.8 ± 1.01
C5	**2.3**	**4.5**	210.3 ± 1.25	0.513 ± 0.02	73.1 ± 1.10	14.67 ± 0.60	22.2 ± 1.08
C6	**6.6**	**4.5**	188.9 ± 2.02	0.433 ± 0.01	75.8 ± 1.40	15.27 ± 0.57	24.5 ± 1.27
C7	**4.5**	**3.7**	123.5 ± 1.76	0.346 ± 0.02	79.7 ± 1.16	16.97 ± 0.78	27.6 ± 0.75
C8	**4.5**	**5.2**	148.6 ± 2.46	0.384 ± 0.01	82.6 ± 1.12	18.43 ± 0.68	29.6 ± 0.80
C9	**4.5**	**4.5**	112.6 ± 1.15	0.401 ± 0.01	81.2 ± 1.11	18.33 ± 0.87	25.9 ± 0.30

Table 5: ANOVA for dependent variables.					
Source	**Sum of Squares**	**Degrees of Freedom**	**Mean Square**	**F Value**	**P Value**
For Y1 = Particle size (nm)					
Regression	8228.62	5	1645.72	100.39	0.0015
Residual	49.18	3	16.39	-	-
Total	8277.80	8	-	-	-
For Y2 = PDI					
Regression	0.0202	5	0.0040	35.97	0.0070
Residual	0.0003	3	0.0001	-	-
Total	0.0206	8	-	-	-
For Y3 = % Entrapment efficiency					
Regression	71.29	5	14.26	148.67	0.0009
Residual	0.2877	3	0.0959	-	-
Total	71.58	8	-	-	-

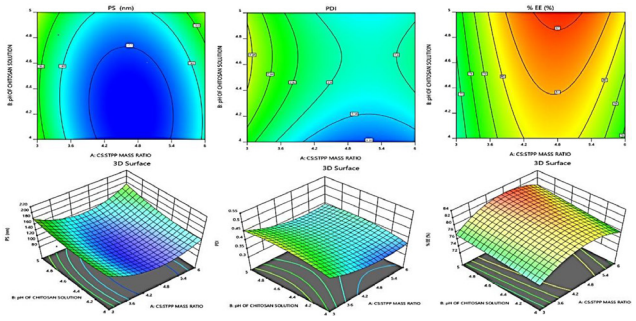

Figure 2: Contour plots and 3D surface plots generated from the central composite design demonstrating the effect of CS: STPP mass ratio and chitosan solution pH on the chitosan nanoparticles diameter, PDI and % EE.

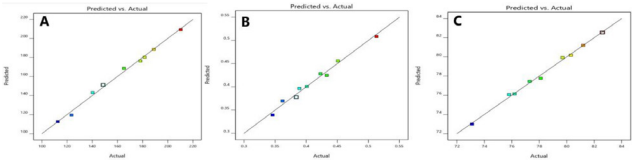

Figure 3: A) Actual and predicted values for PS, B) Actual and predicted values for PDI, C) Actual and predicted values for % EE.

The predicted vs actual graphs quantitatively assess the experimental response values to the predicted values from the constructed models.[43-44] Figure 3 shows that the experimental and predicted findings have a higher correlation and agreement.

Check points analysis, model validation and selection of optimized formulation

As illustrated in Figure 4, two check point batches were developed for the validation of response surface methodology.

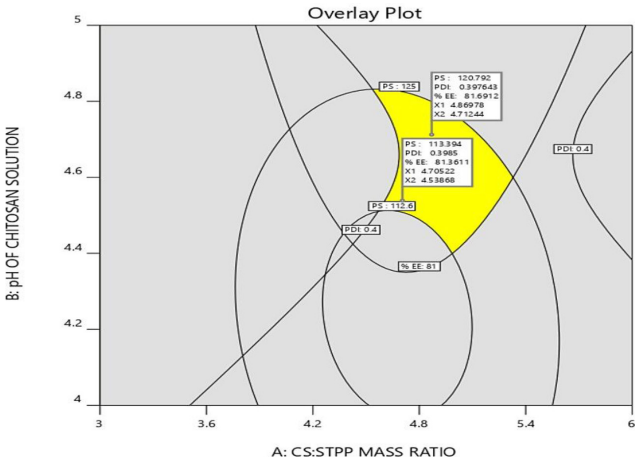

Figure 4: Overlay plot of responses for all dependent variables.

As indicated in Table 6, the actual experimental and predicted responses were compared to validate the design. The dependent variable findings were determined to be within limits for both checkpoint formulations. The experimental values of the responses were correlate to the predicted values to estimate the prediction error of RSM findings. These findings show that the optimization model is accurate in anticipating the impact of process variables on particle size, PDI, and % EE of QU loaded nanoparticles. The formulation F1 was elected as the best optimized formula for QU loaded chitosan nanoparticles as the prediction error was found to be least for the response variables.

Effect of core to coat ratio on chitosan nanoparticles

Table 7 shows the effect of core:coat ratios on PS, PDI % EE, % LC and ZP on chitosan nanoparticles.

Table 6: Composition of optimum check point batches and comparison of experimental and predicted values of response variables (*n*=3, mean ± SD).

Sl. No.	Check point formulations		Response Variables	Experimental values	Predicted values	Prediction error
	X1	X2				
F1	4.70	4.53	Y1	114.2 ± 1.42	113.3	-0.9
			Y2	0.396 ± 0.02	0.398	0.002
			Y3	82.1 ± 1.06	81.3	-0.8
F2	4.86	4.71	Y1	118.6 ± 1.56	120.7	2.1
			Y2	0.401 ± 0.03	0.397	-0.004
			Y3	80.1 ± 1.32	81.6	1.5

Table 7: Effect of core:coat ratio on chitosan nanoparticles (*n*=3, mean ± SD).

Formulation	Core:coat ratio	PS (nm)	PDI	%EE	% LC	ZP
A1	1:2	285.7 ± 1.20	0.391 ± 0.03	79.8 ± 1.55	18.5 ± 0.65	-31.6 ± 1.06
A2	1:3	330.2 ± 0.40	0.412 ± 0.02	80.4 ± 1.66	19.9 ± 0.50	-28.8 ± 1.08
A3	1:4	396.7 ± 1.02	0.365 ± 0.01	78.9 ± 1.76	18.4 ± 0.15	-23.4 ± 0.50
A4	1:5	546.2 ±0.39	0.498 ± 0.01	77.6 ± 1.30	17.3 ± 0.61	-20.3 ± 0.75

Characterization of nanoparticles

Table 4 and Table 7 summarized PS, PDI, % EE, % LC and zeta potential of prepared nanoparticles.

Particle size and Polydispersity index

The largest particle size appeared in C5, 210.3 nm which could be due to lower CS: STPP mass ratio. A related phenomenon has been documented that large diameter aggregates are formed when the mass ratio of CS-STPP is decreased.[45-46] The ability of CS to gel rapidly when it comes into contact with STPP is thought to be due to the development of intermolecular and intramolecular cross links between the amino and phosphate groups. STPP could mainly inter- and intramolecular cross-link with CS to produce tiny nanoparticles if the mass ratio of CS-STPP was high (a little quantity of STPP available). The available quantity of STPP grew as the mass ratio of CS-STPP decreased, and the redundant STPP would connect nanoparticles to produce bigger ones.[47]

Polydispersity index is the measure of particle size homogeneity. PDI indices < 0.5 for most formulations, as evident from Table 3 indicating better monodispersity.[48-49] A narrow size distribution was shown by the values of PDI for ES 100 coated QLCN, which ranged from 0.391-0.498. i.e., < 0.5.[50-51]

Zeta Potential

For C1 to C9 zeta potential values were obtained in the range of +22.2 to +29.6 mV, as illustrated in Table 5. Compact nano aggregates with a positive overall surface charge spontaneously formed when chitosan and STPP were combined in dilute acetic acid, and the intensity of the surface charge was reflected by obtained zeta potential values. Optimised formulation had zeta potential value of +26.[52-53]

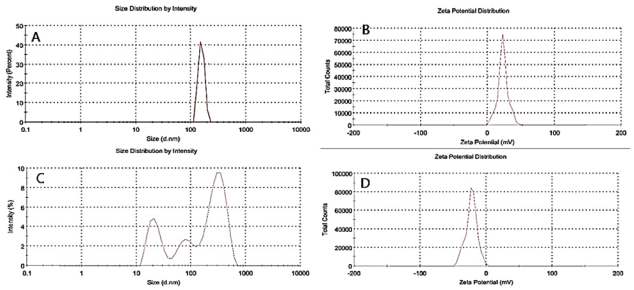

Figure 5: A) Particle size distribution of QLCN, B) Zeta potential of QLCN, C) Particle size distribution of ES 100 coated QLCN, D) Zeta potential of ES 100 coated QLCN.

The negative zeta potential of all ES100 coated QLCN ranged from 20.3 ± 4.78 to -31.6 ± 5.71 mV. These are owing to the free groups of acrylic acids of ES 100, which act as an anionic polymer.[54] The magnitude of the Zeta potential shows the colloidal system's potential stability.[55] Charged particles having a zeta potential greater than 20 mV in either charge have a considerably reduced chance of aggregation. As a result, all of the nanoparticle formulations studied showed high physical stability.[51] Figure 5 shows the particle size distribution and zeta potential of the optimized batch of QLCN as well as ES 100 coated QLCN.

% Entrapment Efficiency and % Loading capacity

It was observed, % EE and % LC were higher at moderate CS: STPP ratio and pH. When the ratio of chitosan to STPP increased, viscosity of medium also increases due to increased chitosan concentration resulted in decreasing the likelihood of ionic interactions between STPP and chitosan leading to a reduction in % EE and % LC.[37,56]

SEM image

The SEM micrograph of QLCN (Figure 6A and B) shows a somewhat rough surface, but after the ES 100 coating on QLCN, the spherical shape with a smooth surface was seen. Particles seemed to be adequately separated, reducing the risk of aggregation and maintaining nanoparticle stability.[29]

In-vitro drug release of QU from nanoparticles

Using a dialysis bag technique, the drug release behaviour of QLCN and ES 100 coated QLCN was observed (Figure 7).

As earlier mentioned, the release of quercetin from QLCN and ES 100 coated QLCN in different dissolution media was assessed using UV spectrophotometry.

There was a burst release of QU from uncoated nanoparticles initially, followed by a more controlled release was ed. The first burst release of the drug from QLCN might be caused by the massive swelling of CS, which is accountable for the creation of holes on the surface of the and the diffusion of the adsorbed drug through the carrier.[32]

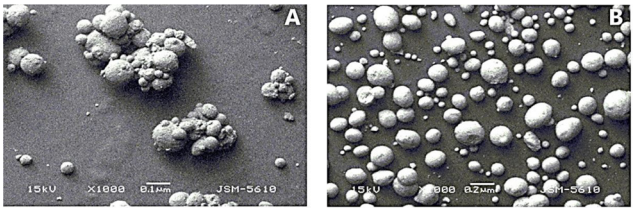

Figure 6: A) SEM image of QLCN, B) SEM image of ES 100 coated CS nanoparticles.

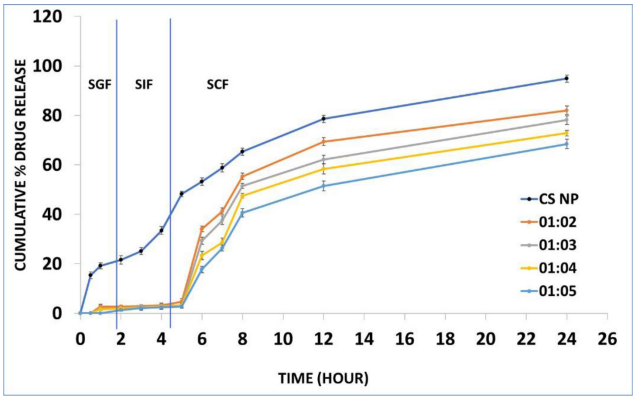

Figure 7: *In-vitro* drug release of QU from nanoparticles.

The initial drug release was minimal (maximum 2.73%) for the eudragit coated nanoparticles up to 2 hr at pH 1.2, suggesting that QU was not released at stomach pH from coated nanoparticles, as contrast to the uncoated nanoparticles, which showed a release 21.65 ± 1.70% at the end of 2 hr.

The minor quantity of drug released from the coated nanoparticles after 2 hr might be accredited to the drug adsorbed on the surface of the nanoparticles. Only a trace quantity of QU was released from coated nanoparticles at pH 6.8 (< 5%) for up to 5 hr, compared to that released from uncoated nanoparticles (48.24%). The drug release from nanoparticles at pH 6.8 might be attributed to pore development after polymer swelling.[57] Since Eudragit S100 is an acrylic polymer that dissolves quickly after de-protonation of carboxyl groups at pH > 7, a significant amount of QU was released from coated nanoparticles at a colonic pH of 7.4.

As a consequence, results revealed that eudragit coated nanoparticles may prevent the drug from being released before it reached the colon, signaling a promising future for colon-specific controlled drug delivery.

Kinetic Modeling

The dissolution profiles were fitted to several models, and the release data collected was analysed using zero order, first order, Higuchi kinetics, Hixson-crowell kinetics, and the Korsmeyer Peppas equation. The resulting plots were developed: Cumulative % DR vs. time (zero order); log cumulative % of drug remaining vs. time (first order); cumulative % DR vs. square root of time (higuchi); cube root % drug remaining in matrix vs. time (hixson-crowell cube root law); and log cumulative % DR vs. log time (korsmeyer peppas model). Coefficients of correlation (R^2) were used to assess the accuracy of the model. Table 8 shows the R^2 values for various kinetic models.

According to the QU release profile from NPs, the Higuchi model is best suited for the drug's release kinetics since it demonstrated a greater value of R^2 from both uncoated and coated formulations (ES 100 coated QLCN and QLCN). The release exponent values for sustained release of QU from QLCN were reported to be 0.515 and >1 for ES 100 coated QLCN. The release exponent strongly suggests that anomalous diffusion (non-Fickian model) is the primary mechanism for releasing QU from Nanoparticles, because of the combined effect of diffusion (due to swelling) and erosion for drug release, and super caseII diffusion kinetics suggest swelling and polymer relaxation.[41,58]

Table 8: Kinetic modelling for QLCN and ES 100 coated QLCN.						
Batch no.	Zero order kinetics	First order kinetics	Higuchi kinetics	Hixson-Crowell kinetics	Korsmeyer Peppas kinetics	
	R^2	R^2	R^2	R^2	R^2	n
A1	0.833	0.911	**0.975**	0.888	0.967	0.515
A2	0.944	0.494	**0.984**	0.816	0.925	1.096
A3	0.670	0.876	**0.965**	0.814	0.890	1.102
A4	0.514	0.767	**0.986**	0.670	0.794	1.076
A5	0.473	0.709	**0.993**	0.623	0.726	1.028

CONCLUSION

According to the findings, colon targeted nanoparticles of Quercetin were effectively produced using the ionic gelation process, followed by coating with ES 100 using the oil in oil solvent evaporation method. Controlled drug release in the colon was demonstrated by *in vitro* drug release study. According to the morphological examination, QLCN has a somewhat rough surface, but ES 100 coated QLCN has a smooth surface. The Higuchi model, which displays super case II diffusion kinetics and suggests swelling and relaxation of the polymer, was best matched to the drug's release mechanism. The developed formulation of QU with pH-stimulated delivery is a viable strategy for drug targeting to the colon.

CONFLICT OF INTEREST

The authors declare that there is no conflict of interest.

ABBREVIATIONS

QU: Quercetin; **QLCN:** Quercetin loaded chitosan nanoparticles; ES 100: Eudragit S 100; **PS:** Particle size; **PDI:** Polydispersity index; **EE:** Entrapment efficiency; **STPP:** Sodium tripolyphosphate; **SGF:** Simulated gastric fluid; **SCF:** Simulated colonic fluid.

REFERENCES

1. Bellik Y, Hammoudi SM, Abdellah F, Iguer-Ouada M, Boukraâ L. Phytochemicals to prevent inflammation and allergy. Recent Pat Inflamm Allergy Drug Discov. 2012;6(2):147-58. doi: 10.2174/187221312800166886, PMID 22352960.
2. Kim YS, Young MR, Bobe G, Colburn NH, Milner JA. Bioactive food components, inflammatory targets, and cancer prevention. Cancer Prev Res (Phila). 2009;2(3):200-8. doi: 10.1158/1940-6207.CAPR-08-0141, PMID 19258539.
3. Lesjak M, Beara I, Simin N, Pintać D, Majkić T, Bekvalac K, *et al*. Antioxidant and anti-inflammatory activities of quercetin and its derivatives. J Funct Foods. 2018;40:68-75. doi: 10.1016/j.jff.2017.10.047.
4. Haytowitz DB, Wu X, Bhagwat S. USDA database for the flavonoid content of selected foods, release. United States Department of Agriculture; 2018. p. 173.
5. Boots AW, Haenen GR, Bast A. Health effects of quercetin: From antioxidant to nutraceutical. Eur J Pharmacol. 2008;585(2-3):325-37. doi: 10.1016/j.ejphar.2008.03.008, PMID 18417116.
6. Dajas F. Life or death: Neuroprotective and anticancer effects of quercetin. J Ethnopharmacol. 2012;143(2):383-96. doi: 10.1016/j.jep.2012.07.005, PMID 22820241.
7. D'Andrea G. Quercetin: A flavonol with multifaceted therapeutic applications? Fitoterapia. 2015;106:256-71. doi: 10.1016/j.fitote.2015.09.018, PMID 26393898.
8. Russo M, Spagnuolo C, Tedesco I, Bilotto S, Russo GL. The flavonoid quercetin in disease prevention and therapy: Facts and fancies. Biochem Pharmacol. 2012;83(1):6-15. doi: 10.1016/j.bcp.2011.08.010, PMID 21856292.
9. Serban MC, Sahebkar A, Zanchetti A, Mikhailidis DP, Howard G, Antal D, *et al*. Effects of quercetin on blood pressure: A systematic review and meta-analysis of randomized controlled trials. J Am Heart Assoc. 2016;5(7). doi: 10.1161/JAHA.115.002713, PMID 27405810.
10. Wang W, Sun C, Mao L, Ma P, Liu F, Yang J, *et al*. The biological activities, chemical stability, metabolism and delivery systems of quercetin: A review. Trends Food Sci Technol. 2016;56:21-38. doi: 10.1016/j.tifs.2016.07.004.
11. Harwood M, Danielewska-Nikiel B, Borzelleca JF, Flamm GW, Williams GM, Lines TC. A critical review of the data related to the safety of quercetin and lack of evidence of *in vivo* toxicity, including lack of genotoxic/carcinogenic properties. Food Chem Toxicol. 2007;45(11):2179-205. doi: 10.1016/j.fct.2007.05.015, PMID 17698276.
12. Okamoto T. Safety of quercetin for clinical application (Review). Int J Mol Med. 2005;16(2):275-8. PMID 16012761.
13. Boots AW, Wilms LC, Swennen EL, Kleinjans JC, Bast A, Haenen GR. *In vitro* and *ex vivo* anti-inflammatory activity of quercetin in healthy volunteers. Nutrition. 2008;24(7-8):703-10. doi: 10.1016/j.nut.2008.03.023, PMID 18549926.
14. Kotla NG, Rana S, Sivaraman G, Sunnapu O, Vemula PK, Pandit A, *et al*. Bioresponsive drug delivery systems in intestinal inflammation: State-of-the-art and future perspectives. Adv Drug Deliv Rev. 2019;146:248-66. doi: 10.1016/j.addr.2018.06.021, PMID 29966684.
15. Tang H-Y, Fang Z, Ng K. Dietary fiber-based colon-targeted delivery systems for polyphenols. Trends Food Sci Technol. 2020;100:333-48. doi: 10.1016/j.tifs.2020.04.028.
16. Fang Z, Bhandari B. Encapsulation of polyphenols – a review. Trends Food Sci Technol. 2010;21(10):510-23. doi: 10.1016/j.tifs.2010.08.003.
17. Wang Y, Li J, Li B. Chitin microspheres: A fascinating material with high loading capacity of anthocyanins for colon specific delivery. Food Hydrocoll. 2017;63:293-300. doi: 10.1016/j.foodhyd.2016.09.003.
18. Xiao B, Merlin D. Oral colon-specific therapeutic approaches toward treatment of inflammatory bowel disease. Expert Opin Drug Deliv. 2012;9(11):1393-407. doi: 10.1517/17425247.2012.730517, PMID 23036075.
19. Collnot EM, Ali H, Lehr CM. Nano- and microparticulate drug carriers for targeting of the inflamed intestinal mucosa. J Control Release. 2012;161(2):235-46. doi: 10.1016/j.jconrel.2012.01.028, PMID 22306429.
20. Hua S, Marks E, Schneider JJ, Keely S. Advances in oral nano-delivery systems for colon targeted drug delivery in inflammatory bowel disease: Selective targeting to diseased versus healthy tissue. Nanomedicine. 2015;11(5):1117-32. doi: 10.1016/j.nano.2015.02.018, PMID 25784453.
21. Schmidt C, Lautenschlaeger C, Collnot EM, Schumann M, Bojarski C, Schulzke JD, *et al*. Nano- and microscaled particles for drug targeting to inflamed intestinal mucosa: A first *in vivo* study in human patients. J Control Release. 2013;165(2):139-45. doi: 10.1016/j.jconrel.2012.10.019, PMID 23127508.

22. Torchilin VP. Multifunctional, stimuli-sensitive nanoparticulate systems for drug delivery. Nat Rev Drug Discov. 2014;13(11):813-27. doi: 10.1038/nrd4333, PMID 25287120.
23. Zhang S, Langer R, Traverso G. Nanoparticulate drug delivery systems targeting inflammation for treatment of inflammatory bowel disease. Nano Today. 2017;16:82-96. doi: 10.1016/j.nantod.2017.08.006, PMID 31186671.
24. Casettari L, Illum L. Chitosan in nasal delivery systems for therapeutic drugs. J Control Release. 2014;190:189-200. doi: 10.1016/j.jconrel.2014.05.003, PMID 24818769.
25. Thanou M, Verhoef JC, Junginger HE. Oral drug absorption enhancement by chitosan and its derivatives. Adv Drug Deliv Rev. 2001;52(2):117-26. doi: 10.1016/s0169-409x(01)00231-9, PMID 11718935.
26. Chen S, Guo F, Deng T, Zhu S, Liu W, Zhong H, *et al*. Eudragit S100-coated chitosan nanoparticles co-loading tat for enhanced oral colon absorption of insulin. AAPS PharmSciTech. 2017;18(4):1277-87. doi: 10.1208/s12249-016-0594-z, PMID 27480441.
27. Vemula SK. Formulation and pharmacokinetics of colon-specific double-compression coated mini-tablets: Chronopharmaceutical delivery of ketorolac tromethamine. Int J Pharm. 2015;491(1-2):35-41. doi: 10.1016/j.ijpharm.2015.06.007, PMID 26056929.
28. Zheng AP, Wang JC, Lu WL, Zhang X, Zhang H, Wang XQ, *et al*. Thymopentin-loaded pH-sensitive chitosan nanoparticles for oral administration: Preparation, characterization, and pharmacodynamics. J Nanosci Nanotechnol. 2006;6(9-10):2936-44. doi: 10.1166/jnn.2006.451, PMID 17048501.
29. Milanezi FG, Meireles LM, De Christo Scherer MM, De Oliveira JP, Da Silva AR, De Araujo ML, *et al*. Antioxidant, antimicrobial and cytotoxic activities of gold nanoparticles capped with quercetin. Saudi Pharm J. 2019;27(7):968-74. doi: 10.1016/j.jsps.2019.07.005, PMID 31997903.
30. Gan Q, Wang T. Chitosan nanoparticle as protein delivery carrier-systematic examination of fabrication conditions for efficient loading and release. Colloids Surf B Biointerfaces. 2007;59(1):24-34. doi: 10.1016/j.colsurfb.2007.04.009, PMID 17555948.
31. Calvo P, Remu□□n-L□pez C, Vila-Jato JL, Alonso MJ. Novel hydrophilic chitosan-polyethylene oxide nanoparticles as protein carriers. J Appl Polym Sci. 1997;63(1):125-32. doi: 10.1002/(SICI)1097-4628(19970103)63:1<125::AID-APP13>3.0.CO;2-4.
32. Raj PM, Raj R, Kaul A, Mishra AK, Ram A. Biodistribution and targeting potential assessment of mucoadhesive chitosan nanoparticles designed for ulcerative colitis via scintigraphy. RSC Adv. 2018;8(37):20809-21. doi: 10.1039/C8RA01898G, PMID 35542340.
33. Oosegi T, Onishi H, Machida Y. Novel preparation of enteric-coated chitosan-prednisolone conjugate microspheres and *in vitro* evaluation of their potential as a colonic delivery system. Eur J Pharm Biopharm. 2008;68(2):260-6. doi: 10.1016/j.ejpb.2007.06.016, PMID 17703928.
34. Khatik R, Mishra R, Verma A, Dwivedi P, Kumar V, Gupta V, *et al*. Colon-specific delivery of curcumin by exploiting Eudragit-decorated chitosan nanoparticles *in vitro* and *in vivo*. J Nanopart Res. 2013;15(9). doi: 10.1007/s11051-013-1893-x.
35. Tsai YM, Chien CF, Lin LC, Tsai TH. Curcumin and its nano-formulation: The kinetics of tissue distribution and blood–brain barrier penetration. Int J Pharm. 2011;416(1):331-8. doi: 10.1016/j.ijpharm.2011.06.030, PMID 21729743.
36. Yang T, Choi MK, Cui FD, Kim JS, Chung SJ, Shim CK, *et al*. Preparation and evaluation of paclitaxel-loaded pegylated immunoliposome. J Control Release. 2007;120(3):169-77. doi: 10.1016/j.jconrel.2007.05.011, PMID 17586082.
37. Shukr MH, Ismail S, Ahmed SM. Development and optimization of ezetimibe nanoparticles with improved antihyperlipidemic activity. J Drug Deliv Sci Technol. 2019;49:383-95. doi: 10.1016/j.jddst.2018.12.001.
38. Varshosaz J, Minaiyan M, Khaleghi N. Eudragit nanoparticles loaded with silybin: A detailed study of preparation, freeze-drying condition and *in vitro/in vivo* evaluation. J Microencapsul. 2015;32(3):211-23. doi: 10.3109/02652048.2014.995728, PMID 25561026.
39. Bashardoust N, Jenita JL, Zakeri-Milani P. Preparation and *in vitro* investigation of chitosan compressed tablets for colon targeting. Adv Pharm Bull. 2011;1(2):87-92. doi: 10.5681/apb.2011.013, PMID 24312762.
40. 5. Mathematical models of drug Release 2015:63-86.
41. Costa P, Sousa Lobo JM. Modeling and comparison of dissolution profiles. Eur J Pharm Sci. 2001;13(2):123-33. doi: 10.1016/s0928-0987(01)00095-1, PMID 11297896.
42. Pal R, Panigrahi S, Bhattacharyya D, Chakraborti AS. Characterization of citrate capped gold nanoparticle-quercetin complex: Experimental and quantum chemical approach. J Mol Struct. 2013;1046:153-63. doi: 10.1016/j.molstruc.2013.04.043.
43. Abul Kalam M, Sultana Y, Ali A, Aqil M, Mishra AK, Aljuffali IA, *et al*. J Biomed-Part I: development and optimization of solid-lipid nanoparticles using Box-Behnken statistical design for ocular delivery of gatifloxacin-Part I: Development and optimization of solid-lipid nanoparticles using Box-Behnken statistical design for ocular delivery of gatifloxacin. J Biomed Mater Res A. 2013;101(6):1813-27. doi: 10.1002/jbm.a.34453, PMID 23255511.
44. Ahad A, Aqil M, Kohli K, Sultana Y, Mujeeb M. Enhanced transdermal delivery of an anti-hypertensive agent via nanoethosomes: Statistical optimization, characterization and pharmacokinetic assessment. Int J Pharm. 2013;443(1-2):26-38. doi: 10.1016/j.ijpharm.2013.01.011, PMID 23313344.
45. Wu Y, Yang W, Wang C, Hu J, Fu S. Chitosan nanoparticles as a novel delivery system for ammonium glycyrrhizinate. Int J Pharm. 2005;295(1-2):235-45. doi: 10.1016/j.ijpharm.2005.01.042, PMID 15848008.
46. Xu Y, Du Y. Effect of molecular structure of chitosan on protein delivery properties of chitosan nanoparticles. Int J Pharm. 2003;250(1):215-26. doi: 10.1016/s0378-5173(02)00548-3, PMID 12480287.
47. Hu B, Pan C, Sun Y, Hou Z, Ye H, Zeng X. Optimization of fabrication parameters to produce chitosan-tripolyphosphate nanoparticles for delivery of tea catechins. J Agric Food Chem. 2008;56(16):7451-8. doi: 10.1021/jf801111c, PMID 18627163.
48. Abdel-Hafez SM, Hathout RM, Sammour OA. Towards better modeling of chitosan nanoparticles production: Screening different factors and comparing two experimental designs. Int J Biol Macromol. 2014;64:334-40. doi: 10.1016/j.ijbiomac.2013.11.041, PMID 24355618.
49. Parmar K, Patel J, Sheth N. Self nano-emulsifying drug delivery system for embelin: Design, characterization and *in-vitro* studies. Asian J Pharm Sci. 2015;10(5):396-404. doi: 10.1016/j.ajps.2015.04.006.
50. Kassem AA, Mohsen AM, Ahmed RS, Essam TM. Self-nanoemulsifying drug delivery system (SNEDDS) with enhanced solubilization of nystatin for treatment of oral candidiasis: Design, optimization, *in vitro* and *in vivo* evaluation. J Mol Liq. 2016;218:219-32. doi: 10.1016/j.molliq.2016.02.081.
51. Asfour MH, Mohsen AM. Formulation and evaluation of pH-sensitive rutin nanospheres against colon carcinoma using HCT-116 cell line. J Adv Res. 2018;9:17-26. doi: 10.1016/j.jare.2017.10.003, PMID 30034879.
52. Mazloom F, Masjedi-Arani M, Ghiyasiyan-Arani M, Salavati-Niasari M. Novel sodium dodecyl sulfate-assisted synthesis of Zn3V2O8 nanostructures via a simple route. J Mol Liq. 2016;214:46-53. doi: 10.1016/j.molliq.2015.11.033.
53. Gan Q, Wang T, Cochrane C, McCarron P. Modulation of surface charge, particle size and morphological properties of chitosan-TPP nanoparticles intended for gene delivery. Colloids Surf B Biointerfaces. 2005;44(2-3):65-73. doi: 10.1016/j.colsurfb.2005.06.001, PMID 16024239.
54. Subudhi MB, Jain A, Jain A, Hurkat P, Shilpi S, Gulbake A, *et al*. Eudragit S100 coated citrus pectin nanoparticles for colon targeting of 5-fluorouracil. Materials (Basel). 2015;8(3):832-49. doi: 10.3390/ma8030832, PMID 28787974.
55. Aditya NP, Shim M, Lee I, Lee Y, Im MH, Ko S. Curcumin and genistein coloaded nanostructured lipid carriers: *In vitro* digestion and antiprostate cancer activity. J Agric Food Chem. 2013;61(8):1878-83. doi: 10.1021/jf305143k, PMID 23362941.
56. Panyam J, Labhasetwar V. Biodegradable nanoparticles for drug and gene delivery to cells and tissue. Adv Drug Deliv Rev. 2003;55(3):329-47. doi: 10.1016/s0169-409x(02)00228-4, PMID 12628320.
57. Gaur PK, Mishra S, Bajpai M. Formulation and evaluation of controlled-release of telmisartan microspheres: *In vitro/in vivo* study. J Food Drug Anal. 2014;22(4):542-8. doi: 10.1016/j.jfda.2014.05.001, PMID 28911472.
58. Sampath M, Lakra R, Korrapati P, Sengottuvelan B. Curcumin loaded poly (lactic-co-glycolic) acid nanofiber for the treatment of carcinoma. Colloids Surf B Biointerfaces. 2014;117:128-34. doi: 10.1016/j.colsurfb.2014.02.020, PMID 24646452.

PICTORIAL ABSTRACT

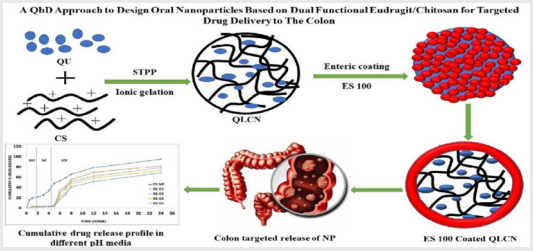

SUMMARY

Ionic gelation method was adopted to prepare QLCN and oil in oil solvent evaporation technique was employed for the coating of QLCN. The resultant nanoparticles were homogenous and spherical in shape with smooth surface, exhibiting a non-Fickian drug release pattern with a colon-targeted drug release profile.

Cite this article: Patel P, Patel T. Design and Development of Dual Functional Colon Targeted Eudragit/Chitosan Nanoparticles: A QbD Approach. Indian J of Pharmaceutical Education and Research. 2022;56(4):1063-75.